



JOINT INSTITUTE FOR NUCLEAR RESEARCH

Frank Laboratory of Neutron Physics, Department of Raman Spectroscopy (Centre “Nanobiophotonics”)

FINAL REPORT ON THE SUMMER STUDENT PROGRAM

Synthesis and up-conversion luminescence studies of phosphors based on $\text{NaYF}_4:\text{Yb}^{3+}, \text{Er}^{3+}, \text{Tm}^{3+}, \text{Yb}^{3+}$ nanocrystals

Supervisor:

Dr. Grigory M. Arzumanyan

Student:

Anka Jevremović,
University of Belgrade, Serbia

Participation periods:

July 01 – July 31, 2018

September 16 – September 28, 2018

Dubna, 2018

Content

1. Abstract	3
2. Introduction	3
2.1. CARS microscopy.....	3
2.1.1. <i>Synthesis of phosphoric materials</i>	4
2.1.2. <i>Experimental: Laser-scanning CARS microscope</i>	4
2.2. Core-shell nanoparticles.....	7
3. Results	8
4. Conclusion.....	11
5. References	13

1. Abstract

Upconversion is a process where low energy light, usually near-infrared (NIR) or infrared (IR), is converted to higher energies, ultraviolet (UV) or visible (VIS), via sequential multiple absorptions. The aim of this work was the synthesis of the phosphors based on $\text{NaYF}_4:\text{Yb}^{3+},\text{Er}^{3+},\text{Tm}^{3+},\text{Yb}^{3+}$ nanocrystals (NCs) and investigation of their up-conversion luminescence properties. The NCs were characterized through the use of transmission electron microscopy and high-resolution luminescence spectroscopy. NCs doped with $\text{Yb}^{3+}\text{Er}^{3+}$ and $\text{Yb}^{3+}\text{Tm}^{3+}$ exhibit green/red and blue upconversion luminescence, respectively.

2. Introduction

2.1. CARS microscopy

Coherent anti-Stokes Raman scattering, a member of the family of coherent nonlinear Raman techniques, was first demonstrated in 1965 at Ford Motor Company (1). In the decade that followed, the technique went by different names, with reference to its place of inception, named it coherent anti-Stokes Raman spectroscopy, or CARS for short (2). In CARS, a pump (ω_p) and a Stokes (ω_s) beam drive the molecular oscillators at the difference frequency $\omega_p - \omega_s$. Under their combined action, a vibrational coherence, a coherent superposition of the ground state and the first excited vibrational state, is created. Through further interaction with the pump beam, the vibrational coherence can be converted into a detectable signal at frequency $2\omega_p - \omega_s$. To express the concept in numbers, in the condensed phase the “excessive feebleness” that Raman described translates into one Raman photon scattered out of 10^{10} incident photons propagating through 1 μm of the Raman active sample (3). To visualize a typical biological specimen with Raman contrast requires long image acquisition times, even when intense laser beams are used. Like spontaneous Raman, CARS probes vibrational modes in molecules and does not require exogenous dyes or markers, which is advantageous in imaging small molecules for which labeling may strongly affect their molecular properties. Second Order Nonlinear Imaging of Chiral Crystals (SONICC) is an emerging technique for crystal imaging based on the second harmonic generation effect found in the majority of protein crystals. CARS signals are 3-4 orders of magnitude stronger than those of a spontaneous Raman process. Another advantage of CARS microscopy is an enhanced spatial resolution which is achieved with two collinearly

overlapping near infrared picosecond beams and a water-immersion objective with a high numerical aperture. Furthermore, the CARS signal is generated only from the focal volume of the objective, thus providing a natural way to perform three-dimensional sectioning without the need of confocal geometry (4,5).

2.1.1. Synthesis of phosphoric materials

Phosphoric materials were prepared by rapid and slow precipitation. A solution of REE with a concentration of 0.2 M (slow synthesis) or by injection (fast synthesis) was added to the 1 M solution of the precipitator (NaF, NH₄F). During the synthesis, an excess of precipitant (F⁻) was used to prepare a single-phase sample. To monitor the morphology of particles and their size, an alcohol solvent was used and was acting as a complexing agent.

2.1.2. Experimental: Laser-scanning CARS microscope

The multimodal optical platform (CARS microscope) for performing transmitted light, Raman, CARS and SONICC imaging is shown in Fig.1.

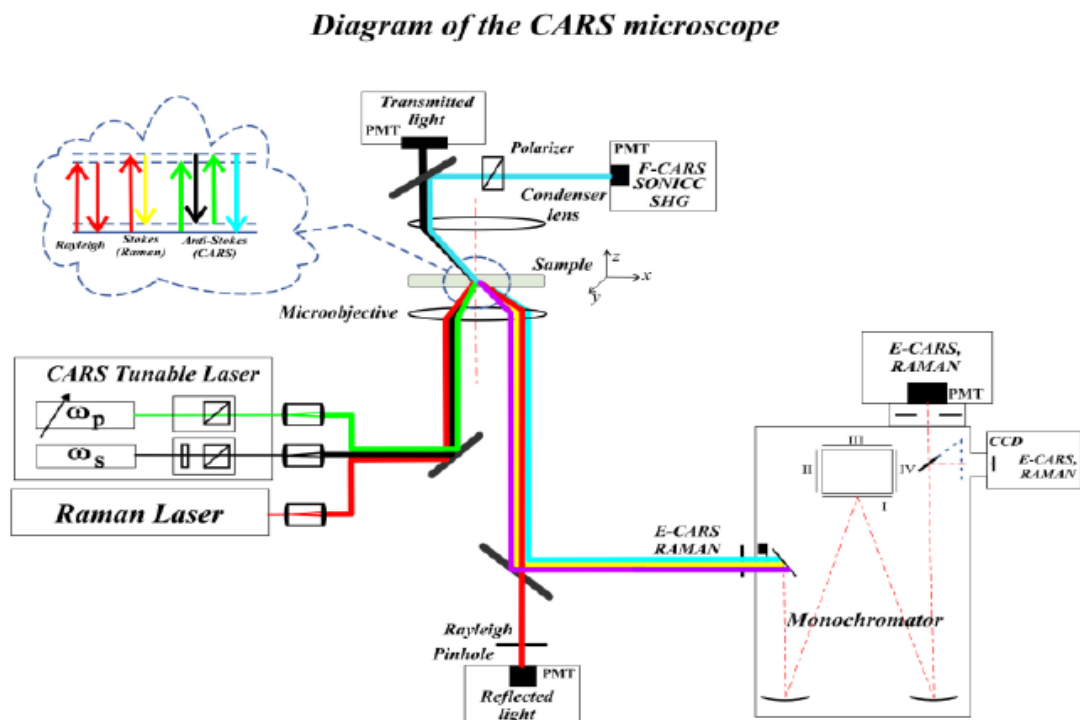
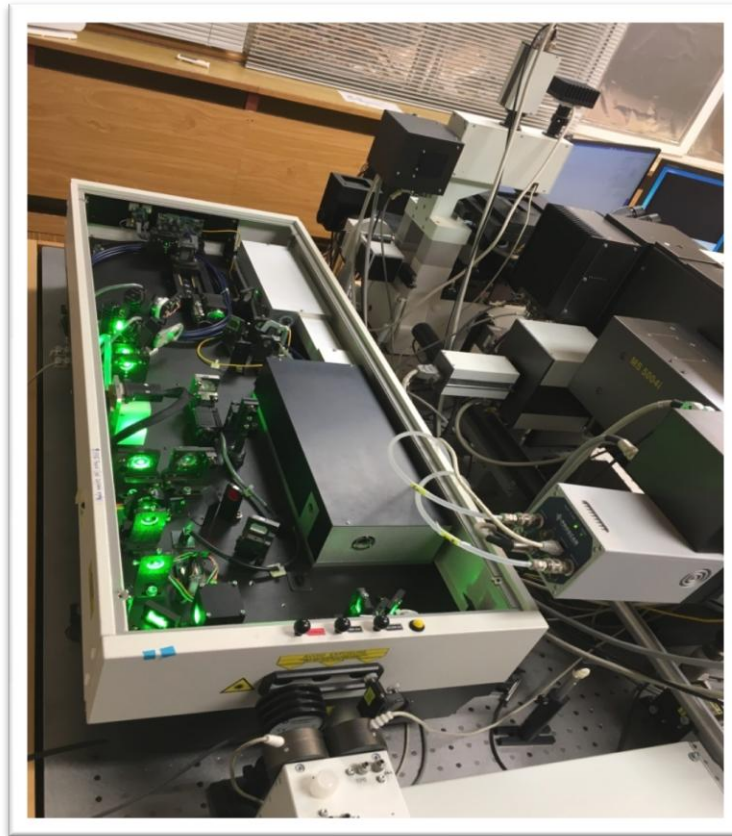


Figure 1. The layout of the multimodal optical platform: “CARS” microscope

It's well-known that the pulse duration of several picoseconds is a proper compromise between high intensity and narrow spectral bandwidth necessary for the CARS microscopy. Besides, its intensity is sufficient also for detection of other nonlinear processes, in particular second and sum harmonic generation. Thus, a picosecond Nd:YVO₄ tunable laser (EKSPLA, PT257-SOPO, Lithuania) with a pulse width of ~6 ps and a repetition rate of 85 MHz is used as the source of the Stokes wave (ω_s) and is simultaneously used to synchronously pump an intracavity-doubled crystal optical parametric oscillator (SOPO). Thereby, the SOPO coherent device provides temporal synchronization with the Nd:YVO₄ and serves as a source of the pump beam (ω_p) tunable from 690 nm to 990 nm with a maximum output power of 300 mW (Fig.2).



(a)



(b)

Figure 2. (a), (b) General view of the CARS microscope

Only a small portion of biologically tolerable laser power is used for CARS and SONICC imaging. The two picosecond laser beams are made coincident in time and in space utilizing an optical delay line and a series of dichroic mirrors. For CARS microscopy, we used an objective lens with a high numerical aperture to focus the beams tightly. With the tight foci, the phase-matching conditions are relaxed because of the large cone of wave vectors of the excitation beams and the short interaction length.

CARS microscopy provides an advanced nondestructive and label-free technique with high sensitivity and high lateral spatial resolution capable of selective chemical imaging of major types of macromolecules: proteins, lipids, nucleic acids, etc. Like spontaneous Raman, CARS probes vibrational modes in molecules and does not require exogenous dyes or markers, which is advantageous in imaging small molecules for which labeling may strongly affect their properties (4).

2.2. Core-shell nanoparticles

Core shell nanoparticles (NPs) are sort of biphasic nanomaterials composed of the inner core and outer shell built by different components (6). The synthesis of core-shell nanoparticles (NPs) has the ability to use a wide range of materials as core or shell that can give a desired and unique properties and functions, such as physicochemical, biological, optical, etc. (7). The core-shell nanoparticles are mainly designed for biomedical applications based on the surface chemistry, which increases its affinity to bind with drugs, receptors, ligands (8, 9). This has led to the synthesis of novel nanoparticles, which in sync with the biological system, compared to bulk material (10-12).

Rare earth (RE) fluorides, mainly REF_3 and $AREF_4$ ($A = \text{alkali}$), have been considered as an excellent starting material thanks to their high refractive index and high transparency arising from low-energy phonons. Those advantages can lead to low probability of nonradiative decay and increased luminescence quantum yield. Although the uses of a conventional organic dye molecule or quantum dot (QD) based biomarker have achieved significant progress in real-time detection and bioimaging, they still have drawbacks. These fluorescent materials are generally excited by ultraviolet (UV) or visible light (VIS), which may induce autofluorescence and photodamage to biological samples, resulting in low signal-to-noise ratio and limited sensitivity. These difficulties have led to development of a new type of high-quality and well-shaped nanomaterials known as upconversion nanomaterials (UCL NPs) which consist of an inorganic host that is doped with Ln^{3+} ions. They show good biocompatibility and generally low cytotoxicity, and are in fact non-cytotoxic to a broad range of cell lines (13, 14).

In order to create high luminescence efficiency, to synthesize high-quality UCNs is not so easy. Therefore, there are three common methods for synthesis UCL NPs: thermal decomposition (15-17), hydrothermal synthesis (18-20), and ionic liquids-based synthesis (21). One of the most popular method is thermal decomposition which can give well shaped particles with good size control including the relatively short period of reaction. It usually requires usage of surfactants with dissolving organic precursors in high-boiling organic solvents.

3. Results

All UCL spectra of synthesized nanoparticles were recorded at room temperature upon laser excitations operating at 633 nm. Samples were illuminated through objective 40x with high numerical aperture. The acquisition time was 1 s.

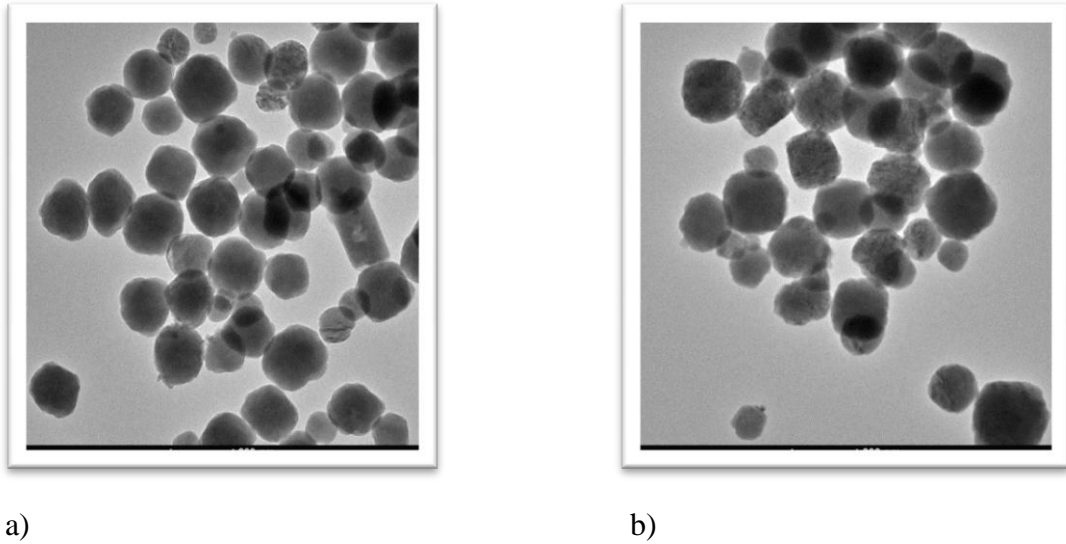


Figure 3. TEM micrographs of phosphors: a) $\text{NaYF}_4:\text{Yb}^{3+}\text{Er}^{3+}$ and b) $\text{NaYF}_4:\text{Yb}^{3+}\text{Tm}^{3+}$

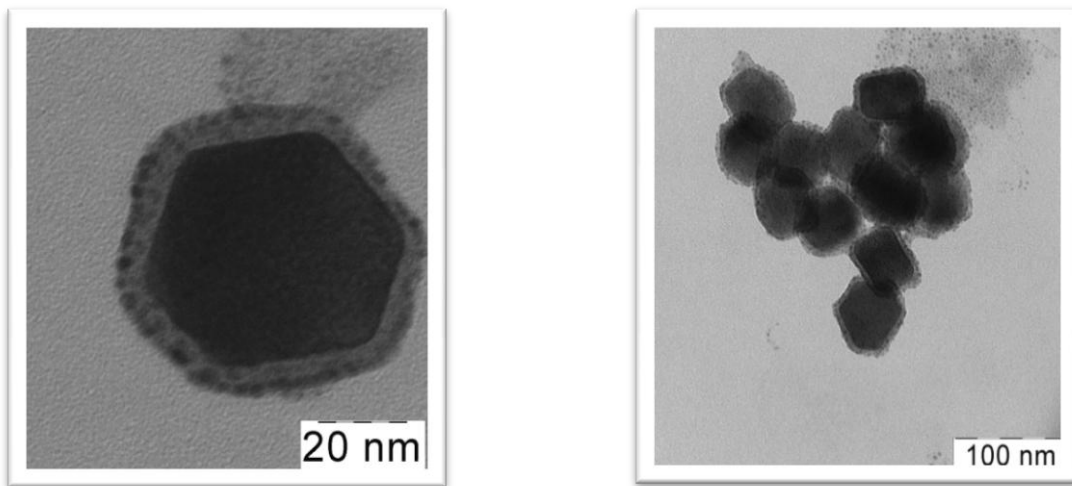


Figure 4. TEM micrographs of core-shell nanoparticles $\text{NaYF}_4:\text{Yb}^{3+},\text{Er}^{3+},\text{Tm}^{3+}@\text{SiO}_2$

In some previous publication, it was found that the synthesis of α -NaYF₄ nanoparticles in octadecene and oleic acid (which was used in this work), resulted in irregularly shaped particles with a wide particle size range (22). From the TEM micrographs we got the modifications made to the earlier synthetic procedure result in nanoparticles with a well defined shape and monodisperse size distribution.

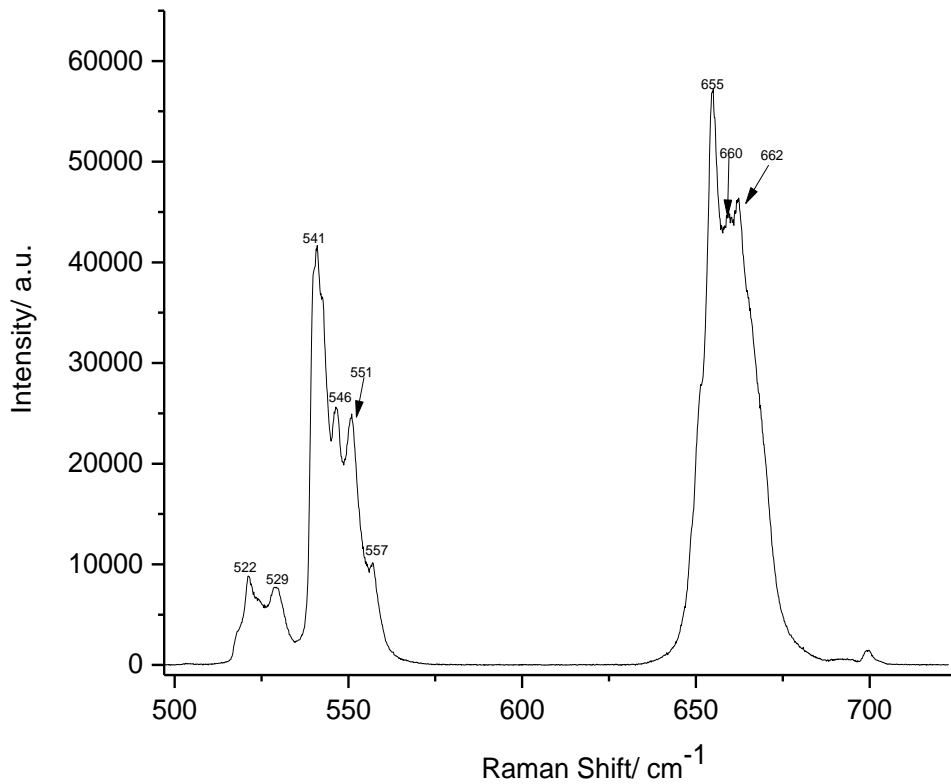


Figure 5. Up-conversion luminescence spectrum of NaYF₄:Yb³⁺Er³⁺

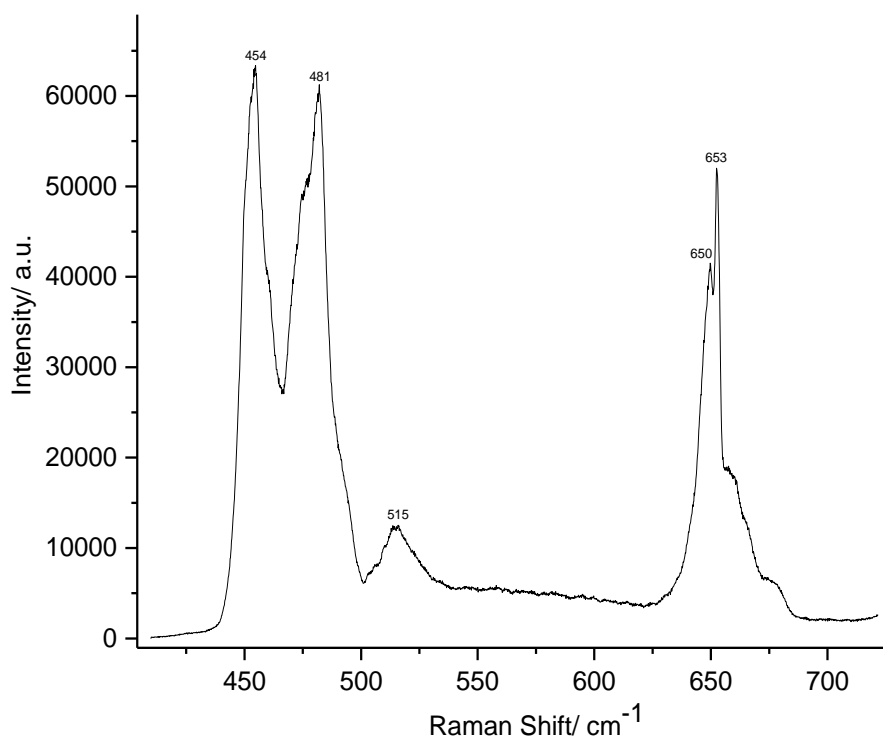


Figure 6. Up-conversion luminescence spectrum of NaYF₄:Yb³⁺Tm³⁺

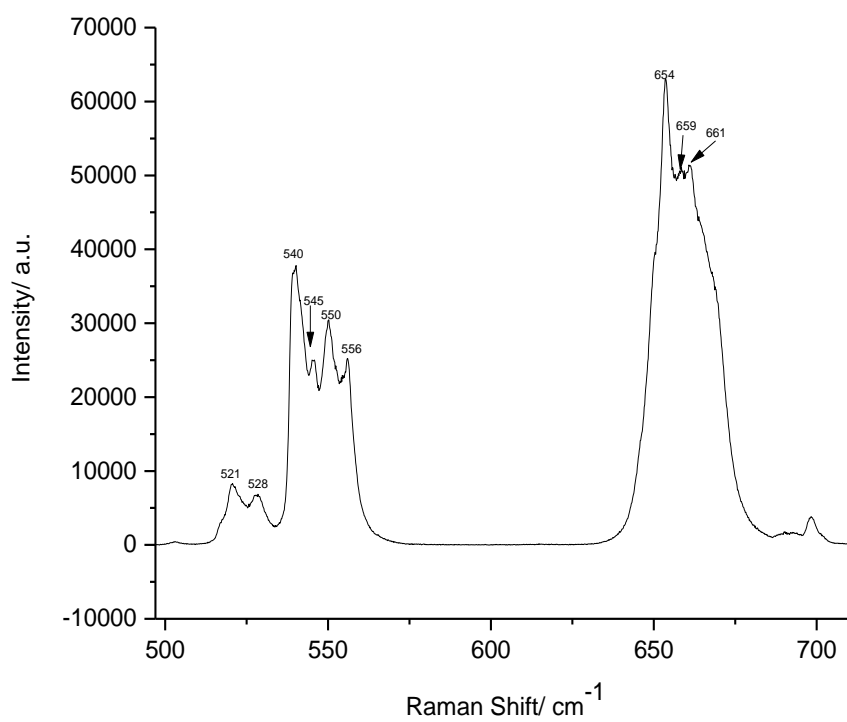


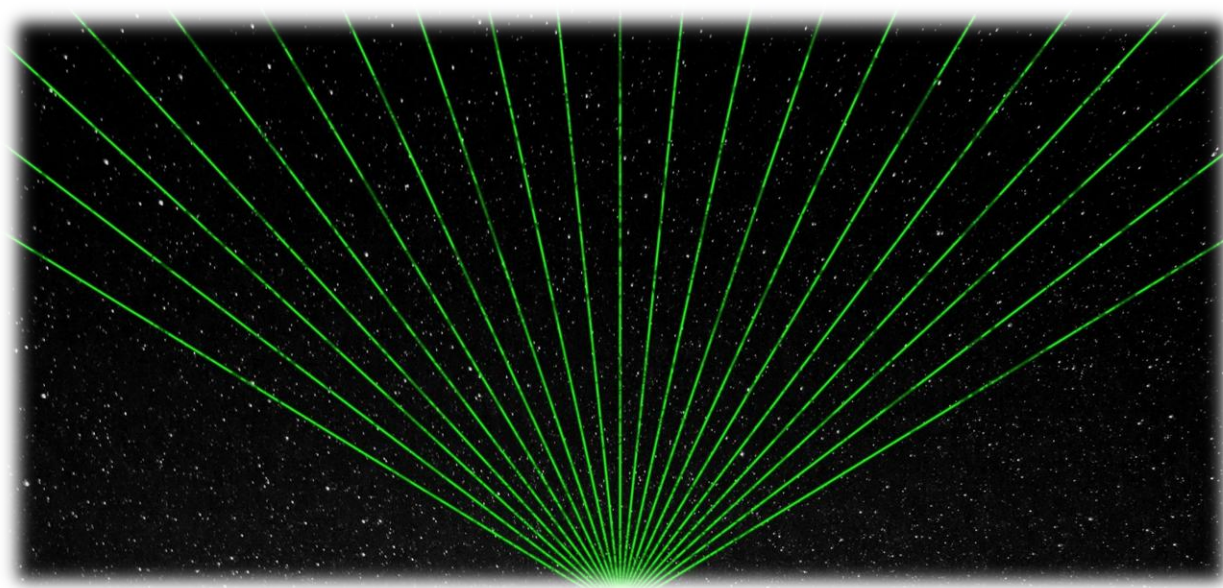
Figure 7. Up-conversion luminescence spectrum of core-shell nanoparticle@SiO₂

4. Conclusion

During the summer student program at Joint Institute for Nuclear Research, I have been acquainted with a unique facility, laser confocal scanning CARS microscope located at the Sector of Raman Spectroscopy, Laboratory of Neutron Physics. Involved in this project I got some experience in advanced methods of nonlinear optical imaging methods, realizing with high contrast and spatial resolution. Besides, I had a good opportunity to learn and experimentally observe the advantages of nonlinear methods in comparison with spontaneous Raman spectroscopy and microscopy.

Work was focused on the synthesis and up-conversion luminescence studies of phosphors based on nanocrystals by laser excitation at 976 nm. It was prepared upconverting lanthanide doped NaYF₄ nanocrystals (NCs) from the thermal decomposition reaction of trifluoroacetate precursors in a mixture of octadecene and oleic acid. We observed and recorded phase transition with different power and exposure time. Also, we started to study core-shell nanoparticles, got the very first preliminary results in which case the further investigation is needed.

I would like to thank to my supervisor, dr Grigory M. Arzumanyan, for his great support, scientific knowlegde, availability and constructive suggestions. It was real honour and privilege to work in his amazing group in Department of Raman Spectroscopy. I would also like to thank to other staff members of this group: Kahramon Mamatkulov, Nelia Doroshkevich, Maria Vorobyova, Anastasia Marchenko and Dimitry Linnik for the confidence and the freedom they gave me to do this work and for providing a so pleasurable and friendly working environment. I am also grateful to University Centre in Joint Institute for Nuclear Research for the chance to be the part of this unforgettable programme.



5. References

1. Maker P. D., Terhune R. W., *Phys. Rev.* **137**, A801-18 (1965).
2. Begley R. F. *et al.*, *Appl. Phys. Lett.* **25**, 387-90 (1974).
3. Bloembergen N., *Proc. Sixth International Conference on Raman Spectroscopy*, Schmid E.D. *et al.*, eds., (Heyden, London, 1978) Vol. 1,335.
4. Zumbusch A., Holtom G., Xie X. *Phys. Rev. Lett.* **82**, 4142–4145 (1999).
5. Krafft C. *et al.* *J. Biophotonics* **2**, 303–12 (2009).
6. López-Lorente A.I., Simonet B.M., Valcárcel M. *Anal. Bioanal. Chem.* **399**,43–54 (2011).
7. Khatami M, Alijani H. Q., Nejad M.S., Varma R.S. *Appl. Sci.* **8** (411), 2-17 (2018).
8. Sahoo S. K, Labhasetwar V. *Drug Discov Today* **8**, 1112–20 (2003).
9. Gilmore J.L, Yi X., Quan L., Kabanov A.V. *J. Neuro. Immune Pharmacol.* **3**, 83–94 (2008).
10. Mahmud A., Xiong X-B., Aliabadi H. M., Lavasanifar A. *J. Drug Target.* **15**, 553–84 (2007).
11. Panda J. J., Mishra A., Basu A., Chauhan V.S. *Biomacromolecules.* **9**, 2244–50 (2008).
12. Van Tomme S. R., Storm G., Hennink W. E. *Int. J. Pharm* **355**, 1–18 (2008).
13. Yang J., Deng Y., Wu Q., Zhou J., Bao H., Li Q., Zhang F., Li F., Tu B., Zhao D. *Langmuir* **26**, 8850-8856 (2010).
14. Zhou J., Sun Y., Du X., Xiong L., Hu H., Li F. *Biomaterials* **31**, 3287-3295 (2010).
15. Li Z., Zhang Y. *Angew. Chem. Int. Ed.* **45**, 7732-7735 (2006).
16. Yi G., Lu H., Zhao S., Ge Y., Yang W., Chen D., Guo L. *Nano Lett.* **4**, 2191-2196 (2004).
17. Boyer J.-C., Cuccia L.A., Capobianco J.A., *Nano Lett.* **7**, 847-852 (2007).
18. Yi G., Sun B., Yang F., Chen D., Zhou Y., Cheng J. *Chem. Mater.* **14**, 2910-2914 (2002).
19. Zeng J.H., Su J., Li Z.H., Yan R.X., Li Y.D. *Adv. Mater.* **17**, 2119-2123 (2005).
20. Taylor J.R., Fang M.M., Nie S. *Anal. Chem.* **72**, 1979-1986 (2000).
21. Wei Y., Lu F., Zhang X., Chen D. *Chem. Mater.* **18**, 5733-5737, (2006).
22. Boyer J.C., Vetrone F., Cuccia L. A., Capobianco J. A. *J. Am. Chem. Soc.* **128** **23**, 7444-7445 (2006).